Multi-species Gyro-kinetic Momentum Transport Modeling with the Trapped Gyro-Landau Fluid Model

G.M. Staebler[1], R.E. Waltz[1], J.E. Kinsey[1], W.M. Solomon[2], and E.A. Belli[1]

[1]*General Atomics, P.O. Box 85608, San Diego, California 92186-5608*
[2]*Princeton Plasma Physics Laboratory, Princeton, New Jersey 08543*

There are a number of mechanisms that can drive momentum transport that have been identified and studied with nonlinear gyro-kinetic simulations. Nonlinear gyro-kinetic simulations of momentum transport due to parallel velocity shear and shear in the $E\times B$ Doppler shift [1,2] have confirmed the discovery from linear theory that these two drives can counteract giving a mechanism for generating intrinsic toroidal flow without external torque [3]. New mechanisms producing momentum transport have recently been discovered: parallel flows [4], the up/down asymmetry of magnetic flux surfaces [5] and the radial variation of the temperature and density gradient lengths [6]. These mechanisms can interact in complex ways that have just begun to be explored [7].

In this paper, the first predictions of toroidal rotation using the quasilinear-trapped gyro-Landau fluid model TGLF [8] will be presented. The TGLF model can include all of the gyro-kinetic drives for momentum transport listed above. However, only a subset will be used for this initial test. The gyro-kinetic theory has been rigorously formulated [9] in the large rotation ordering where the $E\times B$ velocity is one order larger in the expansion parameter (ρ*=gyro-radius/gradient length) compared to the diamagnetic and neoclassical flows. In this ordering, the toroidal $E\times B$ velocity produces a parallel flow and parallel flow shear and a sheared Doppler shift that is related to the parallel flow shear [1]. These three terms are sufficient to self-amplify the boundary toroidal rotation [1,4,7]. The TGLF predicted rotation will be compared with a DIII-D discharge for two times: an unbalanced beam injection phase and a balance bean injection phase with near zero torque.

First, a few details of the momentum transport in TGLF need to be discussed. Including the $E\times B$ Doppler shear in the linear eigenmodes of the gyro-kinetic equation in toroidal geometry has been an outstanding problem [10]. A model for the impact of the $E\times B$ Doppler shear on toroidal eigenmodes was developed for TGLF and fit to nonlinear GYRO [11] simulations. The model [7] conjectured that there is a radial wavenumber induced by the radial variation of the Doppler shift that breaks the poloidal parity. The model for the radial wavenumber was determined by fitting the toroidal Reynolds stress from TGLF to GYRO simulations of a Doppler shear scan. This model has now been validated by direct calculation of the spectral average radial wavenumber of the electric potential fluctuations $\langle k_x \rangle = \left\langle \tilde{\varphi}_{k_y} \middle| i\rho_s \partial/\partial r \middle| \tilde{\varphi}_{k_y} \right\rangle \Big/ \left\langle \tilde{\varphi}_{k_y} \middle| \tilde{\varphi}_{k_y} \right\rangle$. Three cases of this spectral average radial wavenumber $\langle k_x \rangle$

are shown in Fig. 1(a). The bottom curve is for a pure $E\times B$ Doppler shear [1] of γ_{ExB}=0.5. The top curve is for a pure parallel flow shear [1] of γ_p =4.0 and the middle curve is for a GYRO simulation with both terms turned on together. The original TGLF model for k_x [7] was found to be a surprisingly good fit to the computed $\langle k_x \rangle$ for a range of Doppler shear for k_y=0.25-0.75 ($k_y=\rho_s k_\theta$) The model has been slightly refined in order to fit the saturation of $\langle k_x \rangle$ for large Doppler shear. A new model has been added to TGLF that is directly fit to $\langle k_x \rangle$ for the GYRO case with pure parallel velocity shear. The Doppler shear and parallel flow shear contributions are roughly additive as can be deduced from Fig. 1(a) so the TGLF model simply adds the two terms. Note that the two terms partially cancel leaving a negative $\langle k_x \rangle$ for low k_y and a positive $\langle k_x \rangle$ at higher k_y.

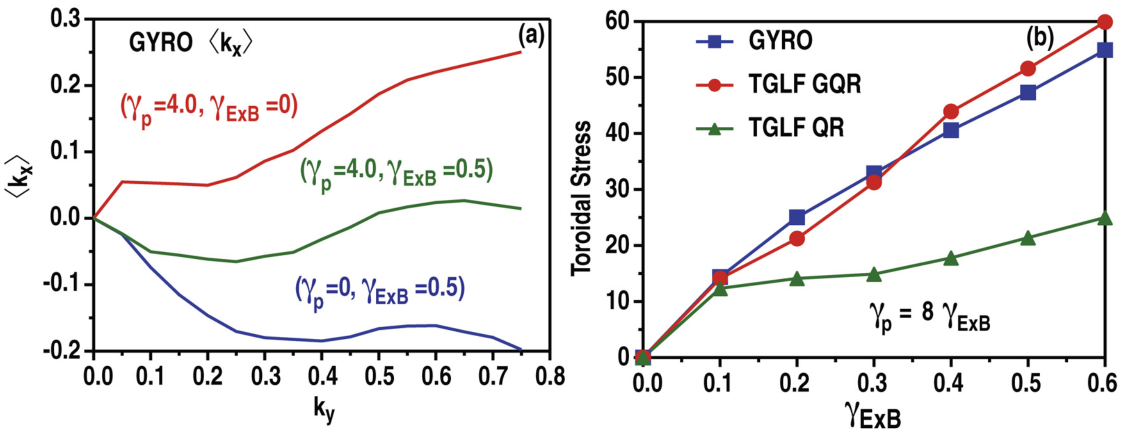

Fig. 1. (a) Spectral average radial wavenumber for the nonlinear electric potential at each k_y for three cases. (b) Toroidal Reynolds stress from TGLF and GYRO vs γ_{ExB} for γ_p =8 γ_{ExB}

This partial cancelation is critical for the net impact on momentum transport as shown in Fig. 1(b). The toroidal stress for TGLF for a scan with γ_p=8 γ_{ExB} is in good agreement with GYRO when the new k_x model is included. The toroidal stess from TGLF using only the original Waltz quench rule (QR) for the Doppler shear gives too much stabilization. In the new generalized quench rule (GQR) [7] part of the stabilization is due to the k_x model. An interesting feature of the GYRO $\langle k_x \rangle$ in Fig. 1(a) is that it vanishes for the zonal flows (k_y=0). Hence, the zonal flows do not make any direct contribution to the poloidal parity breaking or momentum transport.

Turning now to validation with experiment we have chosen two times from DIII-D discharge number 125236. This discharge was part of an experiment on low-torque rotation using opposing directed neutral beams to vary the torque at fixed total power [12]. The discharge is a double-null divertor that is up/down symmetric apart from a slight bias towards the lower divertor. Sawtooth instabilities were avoided using early heating to tailor the safety factor profile. Two times were modeled with TGLF. The early time (2900 ms) has unbalance neutral beam injection in the direction of the torodial current. The later time (3500 ms) has nearly balanced neutral beam injection with a very low torque. TGLF was run to steady state at each time slice in the XPTOR transport code using the heating and fueling sources computed by a ONETWO analysis using a kinetic EFIT (not the same as in Ref. 12). The electron density, electron temperature, ion temperature and $E\times B$ toroidal velocity were evolved. The fast ion density, deuterium density and measured carbon 6+ density were held at a fixed fraction relative to the evolved electron density. The deuterium and carbon were both included in TGLF as a kinetic species. The energy flux for both ion species was added together in the ion energy balance equation. The deuterium and carbon contributions to the toroidal Reynolds stress were added together in the toroidal momentum equation. The self-consistent parallel flow, parallel flow shear and Doppler shear due to the $E\times B$ toroidal rotation were included for all species. A low Mach number approximation is used in TGLF neglecting centrifugal effects. The high accuracy numerical neoclassical code NEO [13] was used. Both ion species were included in NEO. Centrifugal effects are included in NEO in the high $E\times B$ velocity ordering. This is the first time such a comprehensive multi-species, multi-channel simulation of data has been done with TGLF+NEO.

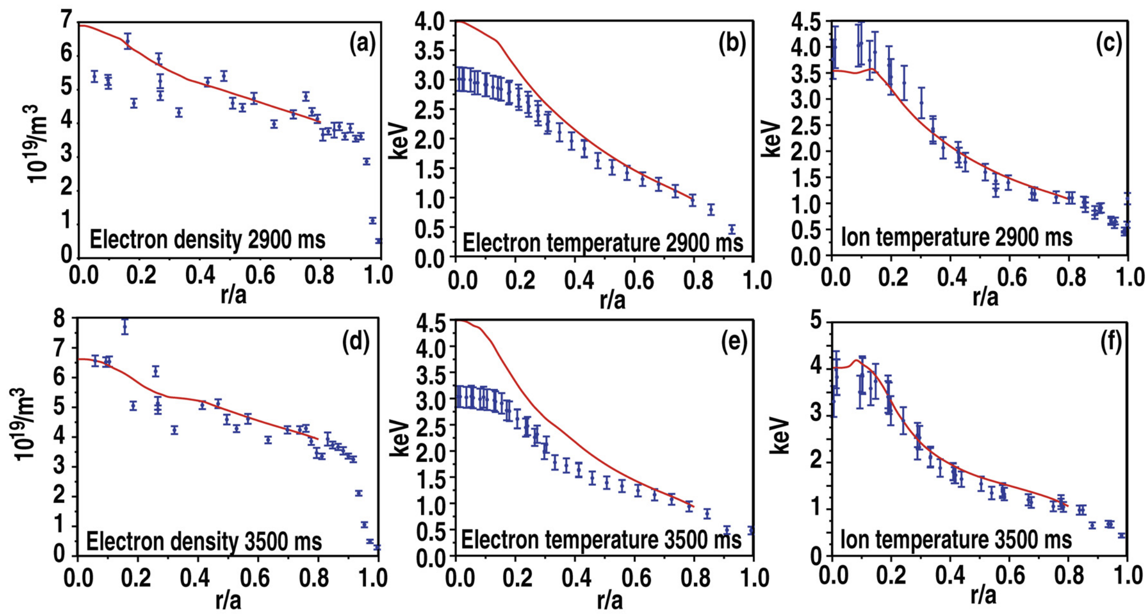

Fig. 2. TGLF predicted (line) and measured (dots) electron density, electron temperature and ion temperature for the co-injected NBI time 2900 ms (a,b,c) and the balanced NBI time 3500 ms (d,e,f) of DIII-D discharge 125236 [12].

The predicted electron density, electron temperature and ion temperature are compared to Thompson scattering, ECE and CER measurements respectively in Fig. 1. The boundary values are taken from experiment at r/a=0.8. Although there are no sawteeth, the TGLF results are sensitive to the uncertain q-profile near the magnetic axis (ρ<0.2). Thus the over-peaking or flattening of profiles in this region should be discounted. Outside ρ=0.2 the agreement is reasonable with the electron temperature showing the largest difference between prediction and data. The predicted toroidal carbon ($E\times B$ only for the assumed ordering) rotation frequency is compared to the measured carbon rotation frequency in Fig. 2. The agreement is good at 2900 [Fig. 3(a)] where there is significant neutral beam torque. The impurity Mach number is approaching 1.0 near the axis but the centrifugal effects on the neoclassical transport are not large. These effects are neglected by TGLF.

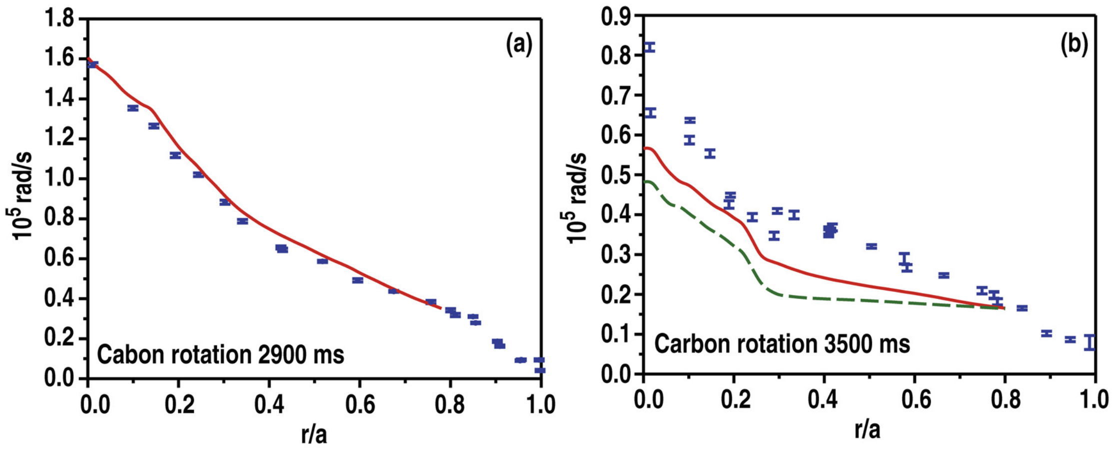

Fig. 3 TGLF predicted (line) and CER measured (dots) carbon toroidal rotation frequency for DIII-D discharge 125236 at (a) 2900 ms and (b) 3500 ms. The predicted carbon rotation without momentum pinch terms (dashed) is shown for reference in (b).

There is a significant amplification of the boundary rotation by the turbulent Reynolds stress at 3500 [Fig. 3(b)] but the level of rotation is lower than measured. Turning off the two momentum pinch effects (parallel flow and Doppler shear induced k_x [7]) gives the dashed line level of rotation in Fig. 3(b) due just to the low net neutral beam torque. For the low torque time (3500), the diamagnetic velocity and neoclassical poloidal flows are not small compared to the $E\times B$ rotation so the large $E\times B$ velocity ordering is violated. This is particularly true near the magnetic axis where the poloidal magnetic field is small. The next step will be to include these flows in the TGLF predictions.

This work was supported by the US Department of Energy under DE-FG02-95ER54309 and DE-AC02-09CH11466.

[1] R.E. Waltz, G.M. Staebler, J. Candy and F.L. Hinton, Phys. Plasmas **14**, 122507 (2007).
[2] F.J. Casson, *et al.,* Phys. Plasmas **16** (2009) 092303.
[3] R.R. Dominguez and G.M. Staebler, Phys. Fluids **B5**, 3876 (1993).
[4] A.G. Peeters, C. Angioni and D. Strintzi, Phys. Rev. Lett. **98**, 265003 (2007).
[5] Y. Camenen, *et al*., Phys. Rev. Lett. **102**, 125001 (2009).
[6] R.E. Waltz, G.M. Staebler and W.M. Solomon, Phys. Plasmas (2011).
[7] G.M. Staebler, J.E. Kinsey and R.E. Waltz, Phys. Plasmas **18**, 056106 (2011).
[8] G.M. Staebler, J.E. Kinsey and R.E. Waltz, Phys. Plasmas **12**, 102508 (2005).
[9] H. Sugama and W. Horton, Phys. Plasmas **5**, 2560 (1998).
[10] J.W. Connor, R.J. Hastie and J.B. Taylor, Plasma Phys. Control. Fusion **46**, B1 (2004).
[11] J. Candy and R.E. Waltz, J. Comput. Phys. **186**, 545 (2003).
[12] W.M. Solomon, *et al.,* Plasma. Phys. Control. Fusion, **49**, B313 (2007).
[13] E. Belli and J. Candy, Plasma Phys. Control. Fusion **50**, 095010 (2008).